NeuroImage 76 (2013) 332–344

Contents lists available at SciVerse ScienceDirect

NeuroImage

journal homepage: www.elsevier.com/locate/ynimg

The effects of aging and Alzheimer's disease on cerebral cortical anatomy: Specificity and differential relationships with cognition

Akram Bakkour [a,c,1], John C. Morris [f], David A. Wolk [g], Bradford C. Dickerson [a,b,c,d,e,*]

[a] Frontotemporal Dementia Unit, Massachusetts General Hospital and Harvard Medical School, Boston, MA, USA
[b] Department of Neurology, Massachusetts General Hospital and Harvard Medical School, Boston, MA, USA
[c] Department of Psychiatry, Massachusetts General Hospital and Harvard Medical School, Boston, MA, USA
[d] Massachusetts Alzheimer's Disease Research Center, Massachusetts General Hospital and Harvard Medical School, Boston, MA, USA
[e] Athinoula A. Martinos Center for Biomedical Imaging, Massachusetts General Hospital and Harvard Medical School, Boston, MA, USA
[f] Department of Neurology and Alzheimer's Disease Research Center, Washington University School of Medicine, St. Louis, MO, USA
[g] Department of Neurology, Alzheimer's Disease Core Center, Penn Memory Center, University of Pennsylvania, Philadelphia, PA, USA

ARTICLE INFO

Article history:
Accepted 25 February 2013
Available online 16 March 2013

Keywords:
Magnetic resonance imaging
Cerebral cortex
Aging
Alzheimer' disease
Parietal lobe
Frontal lobe
Temporal lobe

ABSTRACT

Although both normal aging and Alzheimer's disease (AD) are associated with regional cortical atrophy, few studies have directly compared the spatial patterns and magnitude of effects of these two processes. The extant literature has not addressed two important questions: 1) Is the pattern of age-related cortical atrophy different if cognitively intact elderly individuals with silent AD pathology are excluded? and 2) Does the age- or AD-related atrophy relate to cognitive function? Here we studied 142 young controls, 87 older controls, and 28 mild AD patients. In addition, we studied 35 older controls with neuroimaging data indicating the absence of brain amyloid. Whole-cortex analyses identified regions of interest (ROIs) of cortical atrophy in aging and in AD. Results showed that some regions are predominantly affected by age with relatively little additional atrophy in patients with AD, e.g., calcarine cortex; other regions are predominantly affected by AD with much less of an effect of age, e.g., medial temporal cortex. Finally, other regions are affected by both aging and AD, e.g., dorsolateral prefrontal cortex and inferior parietal lobule. Thus, the processes of aging and AD have both differential and partially overlapping effects on specific regions of the cerebral cortex. In particular, some frontoparietal regions are affected by both processes, most temporal lobe regions are affected much more prominently by AD than aging, while sensorimotor and some prefrontal regions are affected specifically by aging and minimally more by AD. Within normal older adults, atrophy in aging-specific cortical regions relates to cognitive performance, while in AD patients atrophy in AD-specific regions relates to cognitive performance. Further work is warranted to investigate the behavioral and clinical relevance of these findings in additional detail, as well as their histological basis; ROIs generated from the present study could be used strategically in such investigations.

© 2013 Elsevier Inc. All rights reserved.

Introduction

The dementia of Alzheimer's disease is diagnosed when an individual loses independent functioning as a result of impairments in multiple domains of cognitive function (McKhann et al., 1984). These symptoms are thought to be a direct reflection of the loss of function of multiple brain systems for memory, executive function, visuospatial function, language, praxis, and other abilities, and are thought to result, at least in part, from the accrual of pathologic alterations in multiple regions of cerebral cortex (Arnold et al., 1991; Brun and Gustafson, 1976). Analyses of in vivo neuroimaging data demonstrate anatomic and physiologic abnormalities preferentially affecting limbic and heteromodal association cortices (Chetelat et al., 2005; Lerch et al., 2005; Scahill et al., 2002; Thompson et al., 2001; Whitwell et al., 2008). Recently developed computational analytic techniques have enabled the identification of a reliable "cortical signature" of specific regions that undergo atrophy in mild and prodromal AD (Bakkour et al., 2009; Dickerson et al., 2009b). The degree to which this signature atrophy pattern is expressed correlates with symptom severity (Dickerson et al., 2009b), predicts future decline in prodromal patients (Bakkour et al., 2009), and is detectable in cognitively normal individuals with preclinical AD (Dickerson et al., 2011, 2012).

This pattern of AD-related anatomical abnormalities is identified in comparison to cognitively intact individuals of similar age, which presumably controls for atrophy associated with the aging process. Yet it is known that aging itself is associated with regionally specific

* Corresponding author at: MGH Frontotemporal Dementia Unit, 149 13th St., Suite 2691, Charlestown, MA 02129, USA. Fax: +1 617 726 5760.
E-mail address: bradd@nmr.mgh.harvard.edu (B.C. Dickerson).
[1] Present address: Center for Learning and Memory, University of Texas at Austin, Austin, TX, USA.

1053-8119/$ – see front matter © 2013 Elsevier Inc. All rights reserved.
http://dx.doi.org/10.1016/j.neuroimage.2013.02.059

atrophy of the cerebral cortex, most prominently affecting prefrontal, lateral parietal, and sensorimotor regions (Allen et al., 2002, 2005; Brickman et al., 2007; Fjell et al., 2009b; Jernigan et al., 1991b, 2001; Kalpouzos et al., 2009; Raz et al., 1997, 1998, 2004, 2005; Resnick et al., 2003; Salat et al., 2004; Taki et al., 2004; Tisserand et al., 2002; Walhovd et al., 2005). However, a number of inconsistencies are present in the literature regarding the regions within the cerebral cortex that undergo the most substantial atrophy in normal aging, some of which may relate to technical issues related to MRI data acquisition and analytic methodology, and some of which may relate to sample-specific factors such as the presence of subclinical pathology (Raz and Rodrigue, 2006).

Despite observations that aging and AD exert regionally specific effects on the cerebral cortex, and studies demonstrating dissociations between aging and AD in analyses focusing on particular regions of interest (Dickerson et al., 2009a; Head et al., 2005), there has been relatively little comparative investigation of the spatial topographies of these processes surveying the entire cortex (Driscoll et al., 2009; Fjell et al., 2009a, 2010a; Jernigan et al., 1991a,b; McDonald et al., 2009; Ohnishi et al., 2001; Raji et al., 2009). In keeping with the methods at the time, the earlier studies (Jernigan et al., 1991a,b) focused on measurements of the volume of relatively large lobular cortical regions of interest, summarizing for example the parietal cortex and superior occipital cortex as a single measure, the superior posterior region. Ohnishi et al. (2001) performed a very early voxel-based morphometry study directly comparing aging vs. AD and identified several regions as being atrophic in normal aging, including prefrontal and lateral and medial parietal cortex, while the hippocampal formation and MTL cortices were relatively more prominently affected in AD. Raji et al. (2009) found similar results, with the additional observation of relatively prominent primary sensorimotor atrophy in normal aging which had not been observed by the prior studies. In addition, conflicting with Ohnishi, Raji et al. (2009) found that both aging and AD affected the hippocampal body and entorhinal cortex. The first study directly comparing cortical thickness between normal aging and AD focused on a frontostriatal network of regions which was relatively more atrophic in normal aging than a MTL network of regions which was relatively more atrophic in AD (Fjell et al., 2010a). In addition, atrophy of the MTL network was related to cerebrospinal fluid levels of amyloid-β and tau, but the frontostriatal network was not. This study did not compare amyloid-negative older adults to younger adults nor investigate the relationships of structural measures to cognition. Longitudinal investigations, while having the potential to resolve some of the conflicting data identified via the aforementioned cross-sectional studies, have to date only begun to provide novel insights as well as raising additional questions on this point, in part because of the relatively short duration of the initial reports (Driscoll et al., 2009; McDonald et al., 2009).

The existing data leave several important questions only partially answered, which we aimed to address here. First, with a few important exceptions mostly examining specific regions (Raz and Rodrigue, 2006; Rodrigue and Raz, 2004), much of the prior work reporting on differences in cortical structure between older and younger adults has not specifically investigated the relationship of age-related atrophy to cognitive test performance. Second, and perhaps most importantly, to our knowledge there have been no studies published to date that have compared cortical thickness in amyloid-negative cognitively intact older adults to that of young adults. Many cognitively intact older adults harbor AD pathology that is asymptomatic at the time of assessment (Hulette et al., 1998; Price and Morris, 1999; Troncoso et al., 1996). The development of molecular imaging techniques to identify the presence of fibrillar amyloid deposits has demonstrated that approximately 20–30% of cognitively intact adults over the age of 65 harbor silent brain amyloid (Becker et al., 2011; Jack et al. 2012; Mintun et al., 2006; Mormino et al., 2009; Morris et al., 2009), which is thought to be evidence of preclinical AD (Sperling et al., 2011). To date, although there are a growing number of investigations of the localization of cortical atrophy in cognitively normal individuals with brain amyloid (Becker et al., 2011; Chetelat et al., 2010; Dickerson et al., 2009b; Fjell et al., 2010b; Rodrigue et al., 2012), there has been essentially no work to our knowledge on the localization of cortical atrophy in cognitively normal older adults without evidence of brain amyloid, who presumably are experiencing brain changes associated with "normal" aging in the absence of AD pathology. Additional considerations include the following. Although temporal lobe regions, particularly the MTL, appear to be more prominently affected by AD than aging and frontal regions show the opposite pattern, the topography of overlap and lack of overlap in parietal regions is less consistent. Moreover, while the topographic patterns have received investigation, the relative magnitude of atrophy within distinct and overlapping cortical regions has not been reported. Finally, to date, the existing datasets have not been used to generate specific quantitative imaging biomarker summary measures that can be applied to new populations.

In the present study, we set out to systematically compare the spatial topography of cortical atrophy in AD with that of normal aging. Based on our and others' prior work using similar methods of measurement (Dickerson et al., 2009a, 2009b, 2011, 2012; Fjell et al., 2009b; Fjell et al., 2010a; Salat et al., 2004), we hypothesized that there are some cortical regions, such as those in the medial, ventral, and lateral temporal lobe, where the thickness of the cortical ribbon is predominantly affected by AD but much less so by normal aging. Other cortical regions, such as the sensorimotor cortices, were predicted to undergo atrophy in normal aging without appreciable additional atrophy in AD. Finally, frontoparietal cortices were predicted to show a more complex pattern in which some regions are affected much more by one process than the other (e.g., precuneus in AD; inferior frontal gyrus in aging), and some regions are affected by both (e.g., inferior parietal lobule, superior frontal gyrus). To investigate these hypotheses, we further performed specific focused measures of regional cortical thickness across the spectrum of age and AD dementia (young adult/older cognitively intact adult/older adult with mild AD) to determine the localization and relative magnitude of regional atrophy.

We believe there are three major novel contributions of the present work. First, we focused on a group of cognitively intact older adults without brain amyloid in order to determine whether cortical regions thought to be vulnerable to normal aging are substantially affected by aging even in the absence of cerebral amyloid. Second, we specifically examined the relationships of cortical thickness within age- vs. AD-vulnerable regions to cognitive test performance. Finally, in part to lay the foundation for future studies, we generated summary measures of the set of regions identified as being relatively AD-specific vs. those identified as being relatively aging-specific; these summary measures could be used in an unbiased fashion in future studies of normal aging or clinical or preclinical AD.

Participants and methods

Primary sample: participants, clinical assessment, and MRI data acquisition

A primary sample of 257 paid participants (age 18 to 96) was employed in this study. Data from subsets of the participants have been published in previous studies and are available as part of the OASIS sample (http://www.oasis-brains.org/) (Marcus et al., 2007). Four additional samples which are not part of the OASIS sample were also used in this study; one of these samples is described under the amyloid-negative section immediately below. The other three samples, used in the analysis of the similarity of cortical maps described at the end of the Participants and methods section, are detailed in a prior publication (Dickerson et al., 2009b).

Young adults were recruited from the community at Washington University. Non-demented and demented older adults were recruited from the ongoing longitudinal sample of the Washington University AD Research Center (ADRC). All procedures were approved by Washington University's human subjects committee. At study enrollment,

participants were free of non-AD disorders such as major depression, clinical history of stroke, Parkinson disease, and head trauma (Berg et al., 1998).

Trained clinicians assessed each ADRC participant for the presence and severity of dementia based on semi-structured interviews with the research participant and a knowledgeable informant (usually a spouse or adult child) followed by a neurological examination of the participant (Morris, 1993; Morris et al., 1997). The assessment protocol evaluates cognitive problems that represent a decline from a former level of function in daily life for that individual. Also included in the protocol are a health history, depression inventory, aphasia battery, and medication inventory. A psychometric battery is administered to the participants at a separate visit. The CDR staging and clinical diagnostic determinations were made by the examining clinician based solely on the clinical assessment (i.e., without reference to psychometric test results). Diagnostic criteria for AD required the gradual onset and progression of impairment in memory and in at least one other cognitive and functional domain, comparable to standard diagnostic criteria for probable AD (McKhann et al., 1984).

For the purposes of the present study, the resultant clinical diagnostic categories include normal older control (OC, CDR Rating = 0) or mild dementia of the Alzheimer type (referred to here as AD; CDR Rating = 1).

Multiple (three or four) high-resolution structural T1-weighted magnetization-prepared rapid gradient echo (MPRAGE) images were acquired on a 1.5 T Siemens Vision scanner (Siemens Medical Systems, Erlangen, Germany). MPRAGE parameters were empirically optimized for gray–white contrast (repetition time (TR) 9.7 msec, echo time (TE) 4 msec, flip angle (FA) 10, inversion time (TI) 20 msec, delay time (TD) 200 msec, 256 × 256 (1 mm × 1 mm) in-plane resolution, 128 sagittal 1.25 mm slices without gaps, time per acquisition 6.6 min). Participants were provided cushioning, headphones, and a thermoplastic face mask for communication and to minimize head movements. Positioning was low in the head coil (toward the feet) to center the field of view on the cerebral hemispheres.

Amyloid-negative older control sample

Data from an additional sample of non-demented OC participants were analyzed as part of this study (this sample did not include any individuals with AD dementia). This sample consisted of 35 older adults (age range 61–86, 80% females) who were considered to be non-demented OC individuals at the time of MRI scanning; these individuals were recruited, evaluated, and scanned at Washington University as described above. Their data were published previously (Dickerson et al., 2009b). In the initial sample of individuals who underwent amyloid imaging, 35 individuals were amyloid negative and 9 were amyloid positive (the latter not included in the present publication). The proportions of individuals with and without brain amyloid are consistent with other similarly designed studies. In addition to the procedures described above, they were also imaged using [^{11}C]PIB (Klunk et al., 2004) to identify brain amyloid binding. Participants were imaged using [^{11}C] PIB on a 961 ECAT positron emission tomography (PET) scanner (Siemens, Erlangen, Germany) according to the procedures described previously (Buckner et al., 2005; Mintun et al., 2006). PIB-PET imaging provides an in vivo measure of human brain amyloid in plaques associated with AD (Buckner et al., 2005; Klunk et al., 2004; Mintun et al., 2006). Individuals were considered PIB-negative if their binding potential for four cortical regions (prefrontal, lateral temporal, precuneus, and gyrus rectus) was below 0.2 (Fagan et al., 2006; Fotenos et al., 2008; Mintun et al., 2006). For the purposes of the present study, we used PIB-PET imaging to identify 35 older individuals who were cognitively intact and demonstrated no evidence of amyloid deposition. The present classification of participants is the same as that used by previous studies (Andrews-Hanna et al., 2007; Dickerson et al., 2009b; Fotenos et al., 2008).

MRI morphometric data analysis—automated surface reconstruction and alignment of participants

These methods have been previously described in detail (Dale et al., 1999; Fischl and Dale, 2000; Fischl et al., 1999; Kuperberg et al., 2003; Rosas et al., 2002; Salat et al., 2004). The Freesurfer software used to perform the analyses and visualization employed in this study, along with complete documentation, is freely available via the internet at http://surfer.nmr.mgh.harvard.edu. The multiple T1 acquisitions for each participant were motion corrected and averaged to create a single image volume with high contrast-to-noise. The resulting averaged volume was used to segment cerebral white matter (Dale et al., 1999) and multiple subcortical gray matter and ventricular regions (Fischl et al., 2002), and to estimate the location of the gray/white boundary. Topological defects in the gray/white boundary were corrected (Fischl et al., 2001), and this gray/white boundary was used as the starting point for a deformable surface algorithm designed to find the pial surface with submillimeter precision (Fischl and Dale, 2000). Cortical thickness measurements were obtained by calculating the distance between those surfaces at each of approximately 160,000 points (per hemisphere) across the cortical mantle (Fischl and Dale, 2000). The mean thickness of each individual subject's entire cerebral cortex was then calculated. The accuracy of the thickness measures derived from this technique has been previously validated by direct comparisons with manual measures on postmortem brain (Rosas et al., 2002) and on MRI data (Kuperberg et al., 2003). The methods for generation of cortical surfaces and resultant thickness measurements have been shown to be reliable in a test–retest study of a group of older participants scanned twice on the same scanner, as well as across scanner manufacturers and 1.5 T and 3.0 T field strengths (Han et al., 2006), and in a study of different sequence parameters (Wonderlick et al., 2009).

The surface representing the gray–white border was "inflated," differences among individuals in the depth of gyri and sulci were normalized, and each subject's reconstructed brain was then morphed and registered to an average spherical surface representation that optimally aligns sulcal and gyral features across participants. Thickness measures were then mapped to the inflated surface of each participant's reconstructed brain (Fischl et al., 1999). This procedure allows the visualization of data across the entire cortical surface (i.e., both the gyri and sulci) without interference from cortical folding. The data were smoothed on the surface using an iterative nearest-neighbor averaging procedure. One hundred iterations were applied, which is equivalent to applying a 2-dimensional Gaussian smoothing kernel along the cortical surface with a full-width/half-maximum of 18.4 mm. Data were then resampled for participants into a common spherical coordinate system (Fischl et al., 1999). The procedure provides accurate matching of morphologically homologous cortical locations among participants on the basis of each individual's anatomy, while minimizing geometric distortion, resulting in a mean measure of cortical thickness for each group at each point on the reconstructed surface.

MRI morphometric data analysis—exploratory statistical analysis of the entire cortical surface

For the exploratory analysis in the primary sample, two statistical surface maps were generated by computing a two-class general linear model for the effect of membership in 1) the AD group when compared to the OC group and 2) half the OC group when compared to half the YC group on cortical thickness at each point. For these exploratory analyses, a statistical threshold of $p < 10^{-8}$ was used.

MRI morphometric data analysis—generation of cortical ROIs, quantification of magnitude of atrophy, and hypothesis-driven statistical analysis of additional samples

We investigated the magnitude of age-related and AD-related atrophy within cortical regions identified in the two exploratory analyses described above. Nine ROIs known to be affected consistently in AD (Dickerson et al., 2009b) were used in this study. In addition, eight "aging-signature" ROIs were determined based on the exploratory analysis of the first split-half sample of YCs and OCs. For regions in which there was a statistical effect of aging, an ROI label was drawn on the average cortical surface template. These ROI boundaries followed the "aging effects" identified through the exploratory analysis, not gyral or sulcal anatomic boundaries. Aging effects were found to be consistent in the second split-half sample (see end of Results section below).

Fig. 1 shows the statistical AD and aging effects from the exploratory analyses as well as an overlap of the effects of the two processes. The map in Fig. 2 shows ROIs derived from these analyses. Using the spherical registration of each subject to the template, the ROIs were mapped back to individual participants. For each subject, mean cortical thickness within each ROI was calculated by deriving an average of all of the thickness estimates at vertices that fell within the labeled ROI.

For hypothesis-driven analyses, these same 17 ROIs generated from the primary sample were mapped through the spherical registration to each subject, and the mean cortical thickness measures were calculated for each ROI as described above. Thus, the specific location and spatial extent of the ROI was determined a priori from the exploratory analysis of the primary sample and used in subsequent analyses.

For each subject, the resultant ROI measures of cortical thickness were averaged across the two hemispheres, and these 17 values per subject were used for further statistical analysis. These ROI thickness values were used to calculate the mean difference in the thickness of each ROI between the OC and YC groups as well as between the AD and Control groups, the percent atrophy in OCs in relation to YCs as well as ADs in relation to OCs, and the Cohen's *d* effect sizes of aging-related as well as AD-related atrophy for each ROI. Group comparisons were performed using analyses of variance (ANOVA), with a priori-specified planned contrasts, to evaluate differences between OC and YC as well as AD patients and OC. These statistical analyses were performed using SPSS 16.0 (SPSS, Chicago, IL). Note that we use the term "atrophy" in the present study, assuming that cross-sectional cortical thickness differences between older and younger adults or between AD patients and older controls are due to processes associated with cortical thickness shrinkage; although many other investigators use similar terminology, longitudinal methods would likely be the best way to be confident that there are no sample-related or other differences also contributing to cortical thickness differences that are not strictly related to atrophy.

Similarity of effect maps across multiple samples

This analysis was performed to investigate the consistency of the spatial patterns of regional cortical atrophy in normal aging vs. AD. Six maps of atrophy across the entire cerebral cortex were used. First, four independent maps representing AD-related cortical atrophy (AD vs. OC) were obtained from three separate samples of AD and OC, in addition to the sample described above; these samples are described in detail elsewhere (Dickerson et al., 2009b). In addition, two independent maps representing age-related cortical atrophy (OC vs. YC) were obtained from the two split-half samples used in the present study.

The similarity of each map of cortical atrophy to the others was calculated using eta^2 as described previously in detail (Cohen et al., 2008). This is a measure calculated from a pair of maps and indicates the degree of similarity between two maps, with values ranging from 0 (not at all similar) to 1 (identical). The formula computes, on a point-by-point basis, the fraction of the variance in one measure that is accounted for by the variance in another measure, and is equal to:

$$\mathrm{eta}^2 = 1 - \frac{SS_{Within}}{SS_{Total}} = 1 - \frac{\sum_{i=1}^{n}\left[(a_i - m_i)^2 + (b_i - m_i)^2\right]}{\sum_{i=1}^{n}\left[(a_i - \overline{M})^2 + (b_i - \overline{M})^2\right]}$$

where a_i and b_i represent the values at vertex i in maps a and b, respectively. m_i is the mean value of the two maps at vertex i, $(a_i + b_i) / 2$, and M-bar is the grand mean value across all vertices in the map, m, or across all vertices in both maps. eta^2 thus measures the difference in the values at corresponding vertex points in the two maps, not strictly whether the points vary in similar ways, and can detect differences and similarities in the maps using information from all of the vertices of the entire cortical surface. See the prior publication for additional discussion about the value of this measure (Cohen et al., 2008).

Relationship of regional cortical atrophy patterns to cognition

This analysis was performed as an initial investigation of the relevance of cortical atrophy with regard to cognition. For these analyses, we examined the brain-behavior relationships within the two older subject groups—cognitively intact OC and cognitively impaired AD patients—hypothesizing that age-related variation in cognition would relate to thickness in parts of the cortex predominantly affected by aging while AD-related cognitive impairment would relate to atrophy in parts of the cortex predominantly affected by AD.

A total of 87 OCs (mean age = 76.8, CDR = 0, MMSE = 29.1) and 81 AD patients with very mild to mild dementia (mean age = 77.6, CDR = .67, MMSE = 24.6) were included in this analysis. These subjects include all of the OCs and mildly (CDR 1) demented AD patients used in the analysis above plus a group of very mildly demented (CDR 0.5) AD patients (the sample previously published in Dickerson et al. 2009b) to make the OC and AD sample sizes similar for this brain-behavior analysis. Three summary anatomic measures were used: 1) mean cortical thickness across all AD-specific regions, 2) mean cortical thickness across aging-specific regions, and 3) mean cortical thickness across overlap regions that are affected by both AD and aging. The behavioral measure was a summary measure of overall cognitive test performance derived from a factor analysis of performance on a neuropsychological test battery (Kanne et al., 1998; Johnson et al., 2008).

Pearson's correlations of each of the three cortical measures against the general factor were performed in the OC and AD groups separately. Two regression models were constructed in each of the OC and AD groups separately to determine, in each group, which anatomic measure(s) would add the most explanatory power with respect to cognition beyond that explained by demographic measures. The regression analyses were performed by entering three demographic measures—age, gender, and education—into the model in a first block and then including the three anatomical measures in a second stepwise block (p value to enter <0.05).

Results

Participant characteristics

Demographic and clinical characteristics of the participants are presented in Table 1. The AD patients (N = 28) were specifically selected to be relatively homogenous on the basis of a mild level of dementia severity (CDR = 1). MMSE scores (mean = 22.1, S.D. = 3.5) corroborated the relatively mild level of impairment.

The PIB-negative OCs in the second sample (N = 35) were slightly younger than the OCs in the primary sample ($p < 0.01$).

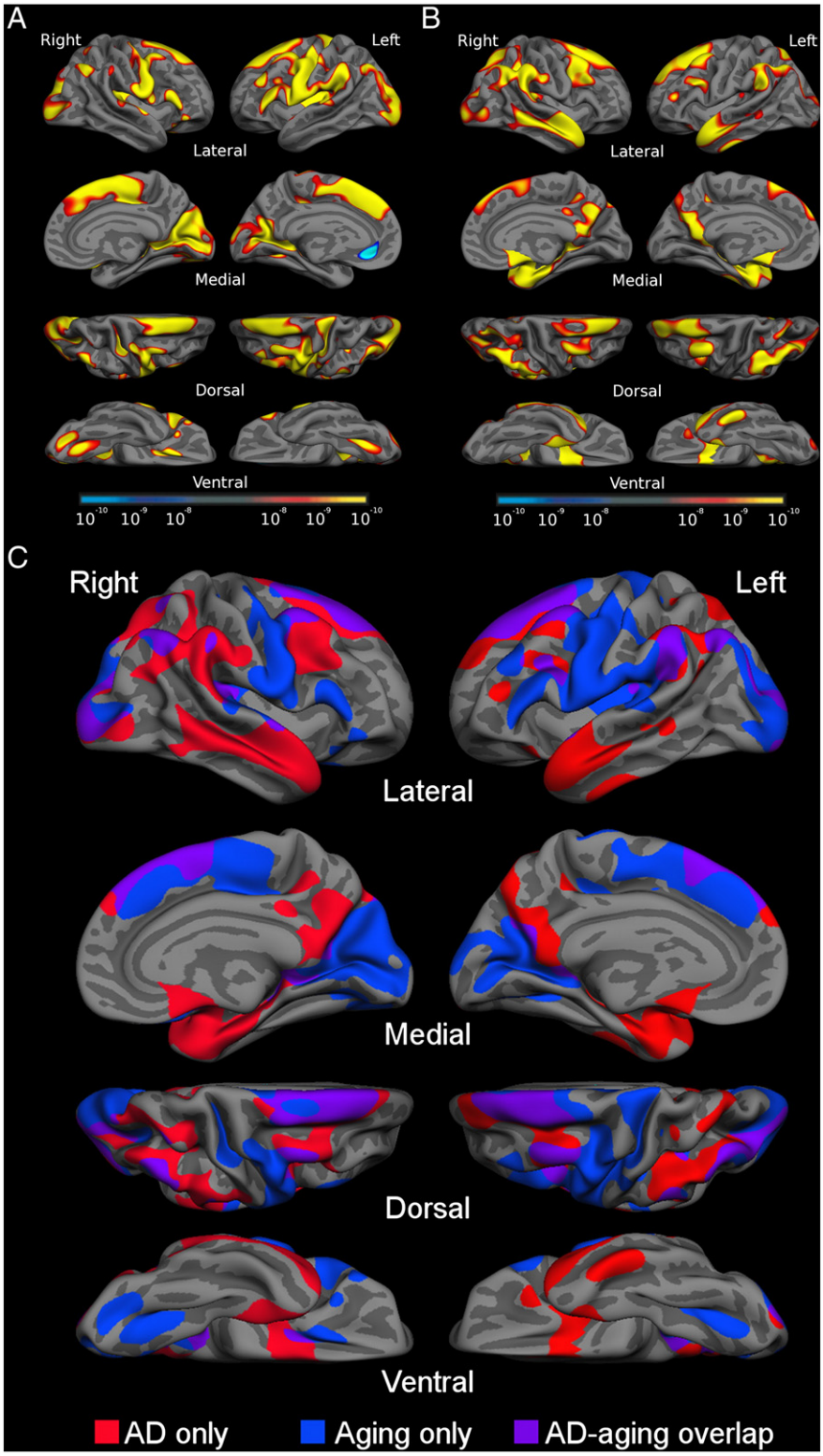

Fig. 1. A) The cortical signature of aging: map of cortical atrophy across the hemispheres in normal aging. B) The cortical signature of AD: map of cortical atrophy across the hemispheres in AD. C) Binarized map showing areas affected by aging only (blue), by AD only (red) and areas affected by both processes (purple). Maps are presented on the semi-inflated cortical surface of an average brain with dark gray regions representing sulci and light gray regions representing gyri. The color scale at the bottom of A and B represents the statistical significance of the thickness difference with yellow indicating regions with smaller p values. See Table 2 for quantitative metrics of the amount of atrophy in each region.

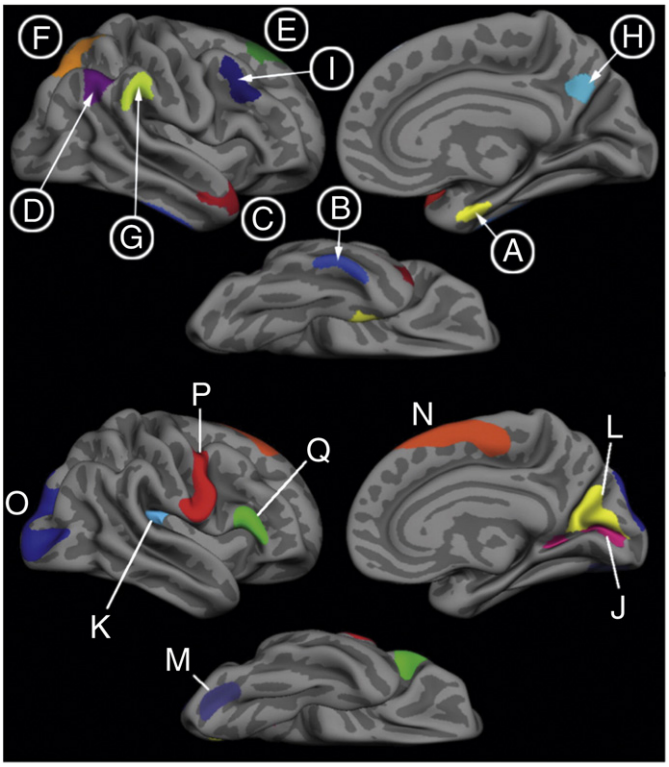

Fig. 2. Top) "AD signature" ROIs. Labels A, B, C, F and H are AD-specific ROIs, where atrophy is seen primarily in AD. Labels D, E, G and I are aging-AD overlap ROIs, where atrophy is seen in both aging and AD. Bottom) "aging-specific" ROIs, where atrophy is seen primarily in normal aging with minimal additional effect of AD.

The spatial topography of cortical atrophy in aging and AD: distinct yet partially overlapping

Analyses comparing the spatial patterns of cortical atrophy in aging vs. AD revealed distinct topographies of regional atrophy in each process, with some areas of overlap. With respect to normal aging, exploratory analyses across the entire cortex demonstrated a set of "aging-signature" regions that were thinner in OC when compared to YC, including occipital (lateral and medial), frontal (precentral, lateral prefrontal, and dorsomedial), and parietal (inferior lateral) cortices, with minimal involvement of the temporal lobe (Fig. 1A). With respect to AD, comparison of AD to OC revealed atrophy in "AD-signature" regions in the temporal (medial, inferior and polar temporal cortices), parietal (superior and inferior lateral and precuneus/posterior cingulate), and prefrontal (mostly lateral superior and middle, as well as ventromedial prefrontal/orbitofrontal) cortices (Fig. 1B).

To directly compare the topography of these two processes, the statistical maps demonstrating AD and aging effects were binarized and displayed on the average brain. Fig. 1C illustrates the regions specifically affected by aging (blue), AD (red), and those that overlap (purple).

Table 1
Demographic and clinical characteristics of participants.

	N	M/F	Age (yrs)		MMSE		CDR	
Group			Mean	S.D.	Mean	S.D.	Mean	S.D.
YC	142	63/79	22.44	3	–	–	–	–
OC	87	23/64	77.68	7.9	28.91	1.2	0	0
AD	28	6/22	77.46	6.6	22.07	3.5	1	0
OCPibneg	35	7/28	73.69	7.5	29.7	0.3	0	0

Values represent mean ± standard deviation.
CDR = Clinical Dementia Rating; MMSE = Mini Mental State Examination; YC = young controls; OC = older controls; OCPibneg = PiB-negative older controls; AD = Alzheimer's disease.

Visual inspection of these patterns indicates that aging has relatively prominent and specific effects on calcarine fissure and cuneus, lateral occipital, dorsomedial prefrontal, inferior frontal, precentral, caudal insula, and caudal fusiform cortex (aging-specific areas). AD, in contrast, has relatively prominent specific effects on medial temporal, inferior temporal, temporal pole, posterior cingulate/precuneus, and superior parietal cortices (AD-specific areas). Areas where both processes are associated with atrophy include supramarginal, angular, lateral superior frontal, and middle frontal cortices (overlap areas).

Cortical regions in which atrophy is predominantly related to the aging process

The area most prominently affected by age and minimally more by AD is the calcarine fissure. The OC group showed 19.6% cortical atrophy in the calcarine compared to YC [YC = 1.84 (S.D. = 0.13) mm, OC = 1.48 (S.D. = 0.14) mm, $F = 403.6$, $p < 0.0001$, Cohen's $d = 2.7$] whereas the AD group exhibited only an additional 6.7% atrophy when compared to the OCs [AD = 1.38 (S.D. = 0.20) mm, $F = 8.4$, $p < 0.005$, Cohen's $d = 0.57$]. Several other regions followed this trend such as the caudal fusiform, caudal insula, cuneus, inferior frontal gyrus, medial superior frontal and precentral cortices showing between 10 and 17.6% atrophy due to aging with only an additional 2.5 to 4.4% atrophy due to AD. Fig. 2 shows the localization of these and other regions and Table 2 presents details of these results.

Cortical thickness measures from these regions that are affected predominantly by aging and only marginally more by AD were averaged to obtain a single measure reflecting the aging process—the aging-specific measure. On this measure, the OCs were 13.3% thinner than the YCs [YC = 2.31 (S.D. = 0.13) mm, OC = 2.01 (S.D. = 0.14) mm, $F = 617.3$, $p < 0.0001$, Cohen's $d = 2.25$] whereas the ADs were only 3.6% thinner than the OCs [AD = 1.94 (S.D. = 0.18) mm, $F = 10.1$, $p < 0.05$, Cohen's $d = 0.43$]. A Z-score of this aging-specific measure was calculated based on the mean and standard deviation of the YCs. Fig. 3A shows that the OCs are 2.4 S.D. thinner than the YC group whereas the ADs are only an additional 0.56 S.D. thinner than the OCs.

Cortical regions in which atrophy is predominantly related to the process of AD

Similar analyses of AD-signature regions demonstrated that AD has prominent effects on medial temporal, inferior temporal, temporal pole, superior parietal, and precuneus cortices, while aging was associated with much lesser effects in these regions. For example, the medial temporal lobe exhibited 12% atrophy when compared to the OCs [OC = 2.85 (S.D. = 0.35) mm, AD = 2.51 (S.D. = 0.32) mm, $F = 20.5$, $p < 0.0001$, Cohen's $d = 1.01$], but only 4.8% atrophy due to aging [YC = 2.99 (S.D. = 0.31) mm, $F = 10.3$, $p < 0.05$, Cohen's $d = 0.43$]. Other regions ranged from 7 to 13% thinner in AD compared to 0.2 to 1.6% thinner in normal aging.

Cortical thickness across these regions affected in AD was averaged to obtain a single AD-specific measure. On this measure ADs were 13.9% thinner than the OC group [OC = 2.46 (S.D. = 0.22) mm, AD = 2.12 (S.D. = 0.26) mm, $F = 54.7$, $p < 0.0001$, Cohen's $d = 1.43$] whereas the OCs were only 5% thinner than the YCs [YC = 2.59 (S.D. = 0.21) mm, $F = 52.6$, $p < 0.0001$, Cohen's $d = 0.60$]. Fig. 3B illustrates that on this measure the OCs are only 0.6 S.D. thinner than the YC group and the ADs are 1.7 S.D. thinner than the OCs.

Cortical regions in which atrophy is related to aging and compounded by AD

Although the processes of aging and AD seem to have largely distinct effects on the cortex, there are a few regions encompassing the inferior parietal lobule and dorsolateral prefrontal cortices that seem to be affected by both processes. A single overlap measure was obtained by

Table 2
Quantitative metrics of atrophy by region within primary sample of participants.

	Region	Mean thickness and SD (mm)						Percent atrophy		Ratio
		YC (N = 142)		OC (N = 87)		AD (N = 28)		OCvsYC	ADvsYC	ADvsOC
Aging	Calcarine	$1.84^{O,A}$	0.13	$1.48^{Y,A}$	0.14	$1.38^{Y,O}$	0.20	19.6	25.0	1.3
	Caudal insula	$2.34^{O,A}$	0.15	1.93^{Y}	0.16	1.86^{Y}	0.21	17.6	20.4	1.2
	Cuneus	$2.01^{O,A}$	0.1	$1.70^{Y,A}$	0.12	$1.63^{Y,O}$	0.12	15.3	19.1	1.2
	Caudal fusiform	$2.01^{O,A}$	0.12	1.76^{Y}	0.16	1.71^{Y}	0.18	12.3	14.8	1.2
	Dorsomedial frontal	$2.99^{O,A}$	0.16	2.65^{Y}	0.16	2.58^{Y}	0.20	11.6	13.8	1.2
	Lateral occipital	$2.08^{O,A}$	0.11	$1.85^{Y,A}$	0.12	$1.79^{Y,O}$	0.19	11.3	14.1	1.2
	Precentral	$2.55^{O,A}$	0.11	$2.27^{Y,A}$	0.14	$2.20^{Y,O}$	0.18	11.0	13.7	1.2
	Inferior frontal	$2.70^{O,A}$	0.15	$2.43^{Y,A}$	0.13	$2.34^{Y,O}$	0.19	10.0	13.2	1.3
AD	Medial temporal	$2.99^{O,A}$	0.31	$2.85^{Y,A}$	0.35	$2.51^{Y,O}$	0.32	4.8	16.1	3.4
	Inferior temporal	2.77^{A}	0.20	2.73^{A}	0.26	$2.36^{Y,O}$	0.23	1.6	14.8	9.4
	Temporal pole	$2.76^{O,A}$	0.22	$2.57^{Y,A}$	0.23	$2.39^{Y,O}$	0.20	6.9	13.5	1.9
	Superior parietal	$2.10^{O,A}$	0.138	$2.00^{Y,A}$	0.13	$1.87^{Y,O}$	0.14	4.7	11.2	2.4
	Precuneus	$2.34^{O,A}$	0.19	$2.17^{Y,A}$	0.14	$2.03^{Y,O}$	0.19	7.5	13.3	1.8
Aging and AD overlap	Angular	$2.58^{O,A}$	0.15	$2.33^{Y,A}$	0.16	$2.09^{Y,O}$	0.24	9.6	19.1	2.0
	Supramarginal	$2.65^{O,A}$	0.17	$2.41^{Y,A}$	0.18	$2.18^{Y,O}$	0.20	9.1	18.0	2.0
	Superior frontal	$2.85^{O,A}$	0.18	$2.57^{Y,A}$	0.18	$2.34^{Y,O}$	0.22	9.8	17.8	1.8
	Middle frontal	$2.36^{O,A}$	0.13	$2.21^{Y,A}$	0.12	$2.01^{Y,O}$	0.15	6.2	14.6	2.4
Mean: entire cortex		$2.34^{O,A}$	0.08	$2.20^{Y,A}$	0.12	$2.05^{Y,O}$	0.11	6.2	12.6	2.0
Mean: aging-specific ROIs		$2.31^{O,A}$	0.13	$2.01^{Y,A}$	0.14	$1.94^{Y,O}$	0.18	13.3	16.4	1.2
Mean: AD-specific ROIs		$2.59^{O,A}$	0.21	$2.46^{Y,A}$	0.22	$2.12^{Y,O}$	0.26	5.0	18.3	3.6
Mean: overlap ROIs		$2.61^{O,A}$	0.16	$2.38^{Y,A}$	0.16	$2.11^{Y,O}$	0.21	8.8	19.3	2.2

YC = young controls; OC = older controls, AD = Alzheimer's disease patients.
$^{Y,O,A}p < 0.05$ different than YC, OC, or AD.

averaging thickness across these regions. On this measure, the OCs were 8.8% thinner than the YCs [YC = 2.61 (S.D. = 0.16) mm, OC = 2.38 (S.D. = 0.16), F = 295.0, $p < 0.0001$, Cohen's $d = 1.45$] and the ADs suffered an additional 11.6% of atrophy compared to the OCs [AD = 2.1 (S.D. = 0.21) mm, F = 31.5, $p < 0.0001$, Cohen's $d = 1.46$]. Fig. 3C illustrates that the OCs are 1.7 S.D. thinner than the YCs and the ADs are an additional 1.0 S.D. thinner than the OC group.

To further understand the effects of aging vs. AD on these cortical regions, a ratio measure was calculated of % atrophy due to AD vs. % atrophy due to aging. Table 2 shows that regions that are affected by AD or that overlap between AD and aging are at least twice as thin in AD as in normal aging (ratios around 2 or greater). Some areas are much more affected by AD than by aging (medial and inferior temporal). In contrast, areas considered to be primarily affected by normal aging show ratios between 1.2 and 1.3, indicating that they are minimally more affected by AD than by normal aging.

Cortical atrophy in amyloid-negative older control individuals

The 35 amyloid-negative OCs (PiB-negative OCs, or OCPibneg) showed a pattern of atrophy strikingly similar to that of the larger OC sample whose amyloid load is unknown. Fig. 3 demonstrates the consistency of the aging effects in the amyloid-negative sample compared to the larger OC group. Aging-specific (OCPibneg = 2.09 (S.D. = 0.15) mm) and overlap areas (OCPibneg = 2.27 (S.D. = 0.15) mm) are affected in a similar manner to that of the normal aging group, while AD-specific areas (OCPibneg = 2.49 (S.D. = 0.24) mm) are relatively spared. These findings reinforce the hypothesis that age-related regional cortical atrophy is not related to possible preclinical AD amyloid pathology.

The magnitude of age-related cortical atrophy is reliable in two separate samples

To ensure that the aging-signature ROIs were affected in a reliable manner, they were derived (as detailed in the Participants and methods section above) from a comparison of OC vs. YC in half of the sample of subjects and then applied in an unbiased fashion to the split-half sample of YCs and OCs. As illustrated in Fig. 4 and Table 3, the effects of aging on the thickness of these regions was remarkably similar in both halves of the sample.

Map-level similarity of atrophy effects within processes and distinction of effects between processes

The eta^2 spatial similarity analysis revealed that the four AD-signature atrophy maps derived from four different samples of OCs and ADs were reasonably similar to each another ($eta^2 = 0.57–0.65$), and the two aging-signature atrophy maps derived from split-half samples of OCs and YCs were very similar to each other ($eta^2 = 0.92$). This is illustrated in the eta^2 matrix in Fig. 6 with the highest values in the upper left (blue-green colors) and lower right (red colors) of the matrix—the within-process relationships. In contrast, the four AD-signature maps are notably different from the two aging-signature maps ($eta^2 = 0.33–0.40$). This analysis quantifies the high degree of reliability of the spatial patterns and magnitudes of atrophy effects within the AD process and the aging process, as well as the differences of these effects between the two processes.

Regionally-specific atrophy due to aging or AD shows distinct relationships to behavior

Within the OC group, the average thickness of the aging-specific cortical regions was correlated with global cognition ($r = .229$, $p < .05$, Fig. 5A). In this OC group, the average thickness of AD-specific or overlap regions did not correlate with this measure of global cognitive function (p values $> .095$). In contrast, in the AD patient group, this same global cognitive measure correlated with the average thickness of AD-specific regions ($r = .414$, $p < .001$, Fig. 5B). Mean cortical thickness among the aging-specific and overlap regions did not correlate with cognition in this group of demented patients (p values $> .3$).

In addition, we performed a multiple linear regression analysis to confirm that the thickness of the relevant cortical areas explained variance over and above that explained by demographic factors, including age, gender and education. This analysis revealed that in the OC group, aging-specific cortical thickness was the only anatomic measure that entered the model to explain additional variance in cognition beyond that explained by demographic factors. Using the demographic measures alone, the regression was significant ($F(3,82) = 6.581$,

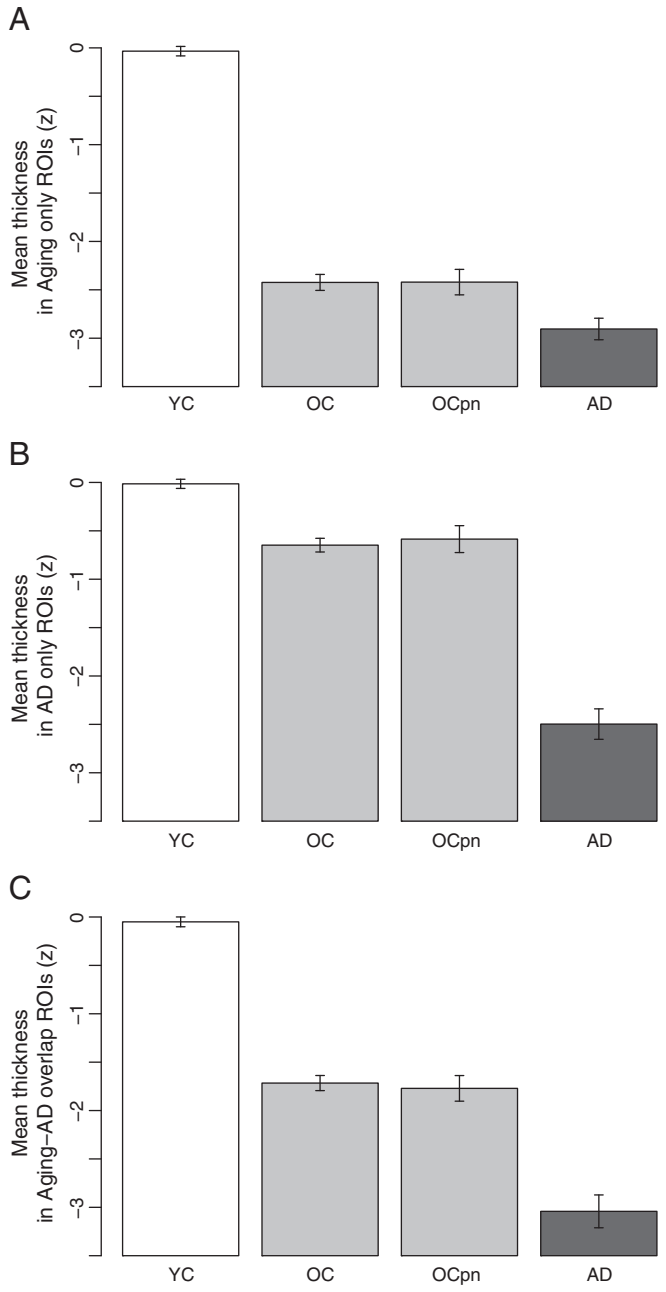

Fig. 3. Mean cortical thickness across A) aging-specific ROIs showing that little additional atrophy is present in AD beyond that of normal aging; B) AD-specific ROIs showing relative sparing of these regions in normal aging and prominent atrophy in AD relative to normal aging; and C) aging-AD overlap ROIs, showing atrophy effects in normal aging and AD of relatively similar magnitude. In all graphs, the group of PiB-PET negative (OCPibneg) individuals is shown to demonstrate that the findings in a group of older adults known not to have amyloid pathology by this marker are very similar to the findings in the larger group of older controls whose pathologic status is unknown, supporting the hypothesis that these are truly age-associated effects. Graphs show mean cortical thickness (z) within each set of ROIs across the four groups, normalized to the young subject group mean. Error bars indicate 1 standard error of the mean. YC: young control; OC: older control; OCPibneg: PiB-negative older control; AD: Alzheimer's disease.

$p < .001$, $R^2 = .165$). Of the demographic predictors only education was significant ($\beta = .395$, $p < .001$, $t = 3.98$). The only anatomical measure that entered the regression after stepwise model selection is aging-specific cortical thickness ($\beta = .249$, $p < .02$, $t = 2.4$), which significantly ($p = 0.018$) improved the model's prediction to $R^2 = .248$.

In contrast, among the AD patients, AD-specific cortical thickness was the only anatomic measure that entered the regression model, explaining additional variance beyond that explained by demographics alone. Using the same three demographic measures alone, the regression was not significant ($F(3,64) = 4.661$, $p > .08$, $R^2 = .098$). No demographic predictors in the first block were significant. The only anatomical measure that entered the regression model after stepwise model selection was AD-specific mean cortical thickness ($\beta = .42$, $p < .001$, $t = 3.77$) which significantly ($p < .001$) improved the model's predictive power to $R^2 = .218$.

These findings show that, in normal aging, differences between individuals in global cognitive performance are largely explained by differences in the thickness of aging-specific cortical regions. In contrast, in AD, differences between individuals in global cognitive performance are largely explained by differences in the thickness of AD-specific cortical regions.

Discussion

The results of the present study, in conjunction with data from previous studies, indicate that the spatial topographies of the processes of aging and AD as they affect the anatomy of the cerebral cortex are largely distinct (Dickerson et al., 2009b; Fjell et al., 2009b; Salat et al., 2004). Although changes in cortical thickness between young adulthood and older age are widespread throughout the cortical mantle, some regions are much more prominently affected than others. Many of these cortical regions that undergo disproportionate age-related atrophy are not those that are most substantially affected by AD, supporting the hypothesis that multiple neural factors contribute to cognitive aging rather than a unitary factor that is differentially expressed (Buckner, 2004; Hedden and Gabrieli, 2004). For example, primary unimodal sensorimotor cortices sustain a large magnitude of age-related atrophy (Fjell et al., 2009b; Good et al., 2001; Lemaitre et al., 2005; Salat et al., 2004), while these areas are minimally affected by neurofibrillary pathology in AD until late in the disease (Arnold et al., 1991; Braak and Braak, 1991; Price et al., 1991), although plaques may be present in these zones (Arnold et al., 1991; Arriagada et al., 1992). The histologic basis of age-related cortical atrophy is not clear, as discussed in greater detail below. Given the differences in spatial distribution of age-related as opposed to AD-related cortical atrophy, along with the confirmation of similar age-related cortical atrophy in a group of older-aged adults without brain amyloid as measured by in vivo PET scanning, it is likely that the biologic basis of age-related atrophy is not preclinical AD pathology. It may be possible to focus future post-mortem studies of age-related cortical abnormalities on regions with the most prominent and specific age effects by using imaging maps as guides to assist pathologists' sampling locations.

In contrast, some areas affected substantially by AD are relatively spared in normal aging, particularly temporal lobe regions. For example, one of the areas that undergoes prominent cortical atrophy in very early AD—the rostral ventromedial temporal lobe within entorhinal and perirhinal cortices—sustains much less prominent (but not negligible) atrophy in normal aging. These areas are cortical regions that, for the most part, are known to harbor greater neurofibrillary than plaque pathology in AD (Arnold et al., 1991). Since some level of neurofibrillary pathology is often found in these areas in non-demented older individuals (Arriagada et al., 1992; Price and Morris, 1999; Price et al., 1991, 2009), it is likely that at least some of the small-to-moderate magnitude atrophy effects found in normal aging occur as a result of neurofibrillary pathology, although this is probably not the only factor. Additional study of the oldest-old in comparison to younger-old individuals may help to shed further light on this issue. An in vivo molecular neuroimaging marker specific to neurofibrillary pathology would be highly valuable in this regard.

Cerebral cortical changes in normal aging

Imaging studies of age-related changes in the cerebral cortex include those using manual region-of-interest approaches and those

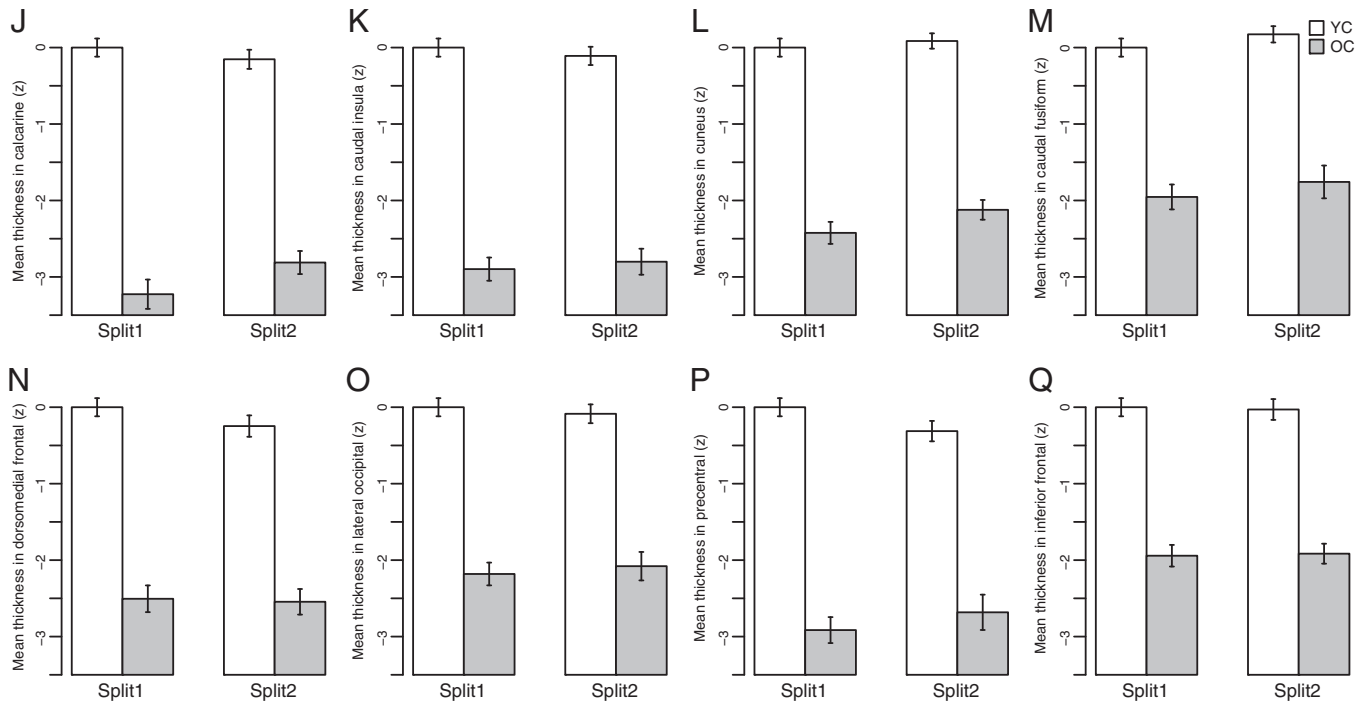

Fig. 4. Mean cortical thickness (z) across the eight "aging-specific" ROIs across both split-half samples of OCs and YCs. The atrophy effect in all aging regions is remarkably similar across the two split half samples. Error bars indicate 1 standard error of the mean.

employing semi-automated or automated methods, which typically survey the spatial distribution of changes throughout relatively large areas of the brain (Brickman et al., 2007; Good et al., 2001; Lemaitre et al., 2005; Ohnishi et al., 2001; Raji et al., 2009; Sato et al., 2003; Smith et al., 2007; Taki et al., 2004; Tisserand et al., 2002). Relatively few studies have directly compared the results of different analytic methods to each other in the same dataset, but those that have done so highlight potentially important differences in results that relate to measurement methodology (Kennedy et al., 2009; Tisserand et al., 2002). The prefrontal cortex is typically highlighted as one of the most consistently affected cortical regions in normal aging, with prominent atrophy in ventrolateral, dorsolateral, dorsomedial prefrontal regions and variable results for ventromedial/orbitofrontal cortices (Fjell et al., 2009b; Raz et al., 1997; Walhovd et al., 2009). Although the results of some studies suggest that primary sensorimotor cortices are relatively spared in normal aging (Jernigan et al., 2001; Raz et al., 1997), a number of recent studies demonstrate that this does not seem to be the case, with precentral, postcentral, Heschl's, and calcarine regions showing fairly prominent age-related atrophy (Fjell et al., 2009b; Good et al., 2001; Resnick et al., 2003; Salat et al., 2004; Smith et al., 2007; Tisserand et al., 2002). In addition, it is worth noting that the caudal insula, a primary viscerosensory region (Craig, 2002), undergoes prominent age-related atrophy that has been reported in figures and tables of prior publications but which has received little discussion (Fjell et al., 2009b). Focused investigation of primary sensory regions of the cerebral cortex with more than one morphometric technique would be valuable given the conflicting results in the literature.

Table 3
Reliability of aging effects within the "aging-signature" ROIs.

Region	Percent atrophy		Effect size	
	Split-half 1	Split-half 2	Split-half 1	Split-half 2
Calcarine	21.35	17.77	2.82	2.60
Caudal insula	18.17	17.00	2.89	2.54
Cuneus	16.09	14.57	2.48	2.61
Caudal fusiform	12.46	12.18	1.88	1.64
Dorsomedial frontal	12.05	11.19	2.31	2.02
Lateral occipital	11.77	10.81	2.20	1.76
Precentral	12.06	9.94	2.74	1.78
Inferior frontal	10.18	9.90	2.00	1.87

Effect size = Cohen's *d* effect size.

From a neuropathological perspective, although there have been a number of post-mortem investigations of the presence, magnitude, and spatial distribution of Alzheimer pathology in non-demented older adults, there has been relatively little study of the regional patterns in the cerebral cortex of other types of changes that accompany aging. A stereologic study of 27 individuals classified as "normal older adults" ranging from 56 to 103 measured cortical thickness, neuronal number, and neuronal density in a region within the superior frontal gyrus and a region within the temporal pole, and also measured these cellular indices as well as area within subfields of the hippocampal formation (Freeman et al., 2008). Analyses were performed within this sample of subjects examining correlations with age. Although cortical atrophy in both regions was identified, with larger frontal than temporal effects, there was no apparent neuronal loss but a slight increase in neuronal density. The authors interpreted their results as supporting suggestions that cortical atrophy in aging is related to the loss of neuropil, which may be driven by age-related reductions in neuronal size, presynaptic terminal numbers, complexity of dendritic arborizations, or possibly gray- or white-matter induced loss of afferent projections (Jacobs et al., 1997; Pakkenberg and Gundersen, 1997).

A very large analysis of in vivo MRI data from six separate samples from North America and Europe focusing on age-related cortical atrophy called attention to the consistency of effects within multiple prefrontal regions, including dorsomedial prefrontal as well as dorsolateral and ventrolateral prefrontal cortex, inferior parietal cortex, and pre- and post-central gyri, results which are consistent with those presented here (Fjell et al., 2009b). Superior and middle temporal gyri, which were not identified as undergoing age-related atrophy in the present investigation, were somewhat inconsistently affected in the previous study except for mid-caudal superior temporal gyrus where age-related atrophy was consistently present. It is possible that at least some of this inconsistency relates to the likely inclusion of variable numbers of individuals in those samples who

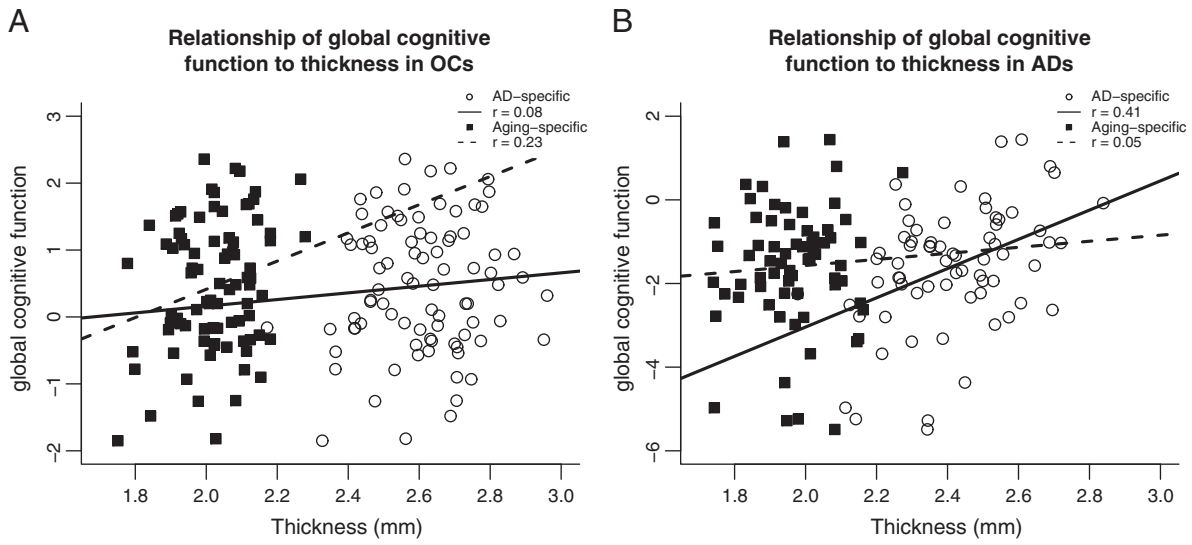

Fig. 5. A) Correlation of the general cognitive factor score with mean cortical thickness across aging-specific regions (squares) and with mean cortical thickness across AD-specific regions (circles) in OCs only. B) Correlation of the general cognitive factor score with mean cortical thickness across aging-specific regions (squares) and with mean cortical thickness across AD-specific regions (circles) in ADs only.

harbored brain amyloid, which was not measureable at the time those scans were acquired. The occipital cortex was less consistently affected across samples in the prior study, although the calcarine fissure itself was an area of reproducible atrophy, again similar to findings presented here. Finally, the polar and ventromedial temporal cortex, precuneus, and anterior cingulate were areas that were consistently relatively spared by normal aging, as we found in the present study.

The relative magnitude of age effects received little attention in the prior study; this was a measure of major interest here given the goal of comparing age-related and AD-related effects directly to each other. On the whole, the cerebral cortex thins by about 6% between young adulthood and older age, but some regions are much more prominently affected beyond this global effect. In the present study, the areas that undergo the most substantial atrophy in normal aging are calcarine fissure, caudal insula, and cuneus (all >15% atrophy). The finding that the cortex within the calcarine fissure undergoes 20% atrophy as part of normal aging is notable because this area is one of the thinnest regions of the entire cortical mantle in young adulthood, as described by Constantin von Economo 80 years ago (von Economo, 2009). The prefrontal cortex also undergoes relatively prominent atrophy in normal aging as has been discussed previously (Buckner, 2004; Raz and Rodrigue, 2006), with multiple regions atrophying by about 10%, most notably dorsomedial, superior, and inferior frontal gyri, with less prominent effects on middle frontal gyrus and minimal atrophy in ventromedial/orbitofrontal cortex, again consistent with recent findings

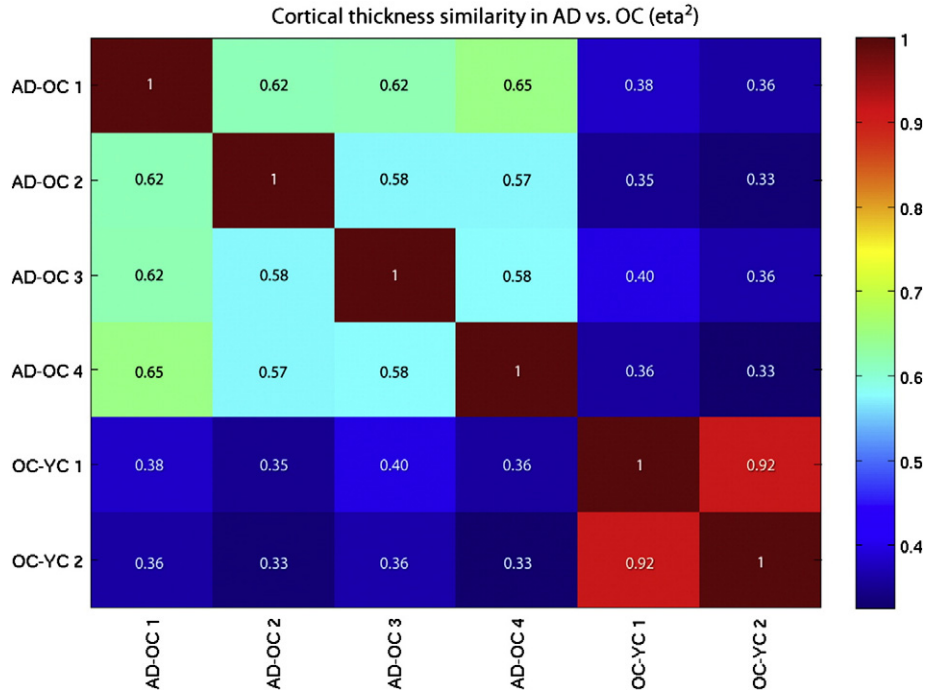

Fig. 6. Eta^2 matrix of similarity of effects between four AD-signature maps and two aging-signature maps.

(Fjell et al., 2009b) and lending support to prefrontal hypotheses of age-related cognitive decline (Buckner, 2004; Raz and Rodrigue, 2006). But the present and previous analyses (Fjell et al., 2009b) of age-related cortical atrophy also show that posterior regions (including inferior parietal lobule, lateral occipital cortex, and caudal fusiform cortex) undergo a similar magnitude of atrophy, findings which run counter to some (Raz and Rodrigue, 2006) but not all (Good et al., 2001) previous investigations. Thus, although relatively large swaths of cortex undergo atrophy in the prefrontal cortex, there are other areas, particularly within occipitoparietal and some sensorimotor cortices, in which the magnitude of age-related atrophy appears to be at least as prominent as that in the prefrontal cortex, providing some support for sensory-cognitive models of aging such as the common cause hypothesis (Lindenberger and Baltes, 1994).

Spatial overlap between aging and AD effects on the cerebral cortex

The findings of the present study indicate that, although aging and AD are associated with atrophy that involves largely spatially distinct regions of the cerebral cortex, there are areas of notable overlap, particularly within dorsolateral prefrontal and inferior parietal cortex. The caudal middle frontal gyrus and dorsolateral superior frontal gyrus are areas affected by both aging and AD, with 6 and 10% atrophy in normal aging and 15 and 18% atrophy in AD, both compared to young adults. Angular and supramarginal gyri demonstrate similar effects. The ratios calculated in Table 2 highlight the observation that there are notable effects of normal aging on these regions, but that AD is associated with an approximate doubling of the atrophy effects of normal aging. We calculated an average measure from these aging-AD overlap regions, and showed that these areas undergo atrophy that is greater than average age-related cortical atrophy (8.8% for these regions vs 6.2% average), but that AD is associated with about twice this effect (19.3%). Thus, although AD exerts a prominent influence on the thickness of these regions of the cortex, aging alone is associated with substantial effects as well. Importantly, these cortical regions are involved in, among other functions, executive/attentional processing, being critical nodes in the executive control (Vincent et al., 2008) or attentional (Corbetta and Shulman, 2002) networks defined using task-related and resting-state functional MRI data. This may explain in part why alterations in complex attention or executive function can be seen in both normal aging as well as AD.

Cerebral cortical changes specific to aging or AD

To understand the processes of normal aging and AD, it is valuable to identify effects of each process that are specific to particular brain regions or networks. With respect to normal aging, there are a number of cortical regions that undergo prominent atrophy but are relatively spared by AD. Table 2 highlights eight cortical regions where there is 10–20% atrophy in normal older adults compared to younger adults. For these regions, ratio measures of relative effects of AD vs. aging range from 1.2 to 1.3, indicating that these areas are minimally more affected in AD than in normal aging. These areas include primary sensorimotor regions (calcarine, precentral, and caudal insula), visual association areas (cuneus, lateral occipital, caudal fusiform), as well as specific prefrontal regions in dorsomedial prefrontal cortex and inferior frontal gyrus, which may relate to executive functions/processing speed/generativity (Stuss and Alexander, 2007) and lexical/attentional/control (Corbetta and Shulman, 2002; Gabrieli et al., 1998; Vincent et al., 2008) changes in normal aging, respectively. As shown in Table 2, an average of these "aging-specific" cortical regional thickness measures supports the finding of relatively prominent atrophy in normal aging (13%)—double the global effect of about 6%—with minimally greater atrophy in AD (an additional 3%), giving a ratio of 1.2. This summary measure may be useful as a marker of the degree to which a sample of older adults expresses cortical changes consistent with normal brain aging, although its generalizability and utility for this purpose deserve further study.

Areas of cortical atrophy specific to AD include ventromedial temporal regions within rostral medial temporal cortex, inferior temporal gyrus, and temporal pole, as well as posterior cingulate/precuneus and superior parietal lobule. These regions thin much more prominently in AD than in aging, and a summary measure of these "AD-specific" regions shows atrophy that is less than the average magnitude of cortical atrophy in normal older adults (5%) but more than triple this magnitude in AD (18%), giving a ratio of 3.6. These regions are part of episodic memory, semantic memory, and executive and visuospatial attentional networks that are typically critically disturbed in the early clinical phases of AD. The use of this summary measure may be of value as an imaging biomarker specific to the process of AD as opposed to normal aging, and deserves further investigation for this purpose.

Distinct relationships of specific regional atrophy to cognition

Although the present brain-behavior analysis was meant to investigate relationships between cortical atrophy and cognition at a global summary level, the specificity of findings underscores the dissociation between the anatomic basis of age- vs. AD-related changes in cognition. In normal older adults, cognitive test performance in a variety of domains—particularly processing speed, executive function, and episodic memory—has declined substantially from that of young adulthood (Buckner, 2004; Hedden and Gabrieli, 2004). Based on the results reported here, one factor that relates to the variability in global cognitive performance in normal older adults is the degree to which cortical atrophy is present in aging-specific regions but not in AD-specific or overlap regions. In contrast, inter-individual differences in cognition in patients with AD, which reflect further impairment in specific domains beyond that of normal aging, are best explained by the degree to which AD-specific cortical regions have undergone atrophy. These findings provide further support for hypotheses that age- and AD-related changes in cognition are distinct in their biological underpinnings.

Conclusions

In summary, the processes of aging and AD have both differential and partially overlapping effects on specific regions of the cerebral cortex. This dissociation is underscored by the subsample in the present study of cognitively normal older adults without appreciable brain amyloid measured with PET scanning. Some frontoparietal regions are affected by both processes, most temporal lobe regions are affected much more prominently by AD than aging, while sensorimotor and some prefrontal regions are affected specifically by aging and minimally more by AD. Within cognitively normal older adults, atrophy in aging-specific cortical regions relates to cognitive performance, while in AD patients atrophy in AD-specific regions relates to cognitive performance. Simple summary measures of these regions may be useful as biomarkers in future studies aiming to investigate the presence or prominence of age- vs. AD-related cortical atrophy.

Acknowledgments

This study was supported by grants from the NIA R01-AG29411, R21-AG29840, P50-AG05134, P50-AG05681, and P01-AG03991, the NCRR P41-RR14075 and U24-RR021382, the Alzheimer's Association, and the Mental Illness and Neuroscience Discovery (MIND) Institute.

We thank the faculty and staff of the Washington University ADRC for participant assessment, and Dr. Mark Mintun who was formerly affiliated with the ADRC's Imaging Core for PiB PET studies. We express special appreciation to the participants in this study and their families for their valuable contributions, without which this research would not have been possible. We also thank Dr. Randy Buckner for

data sharing and helpful comments on a draft of this manuscript, and Mark Hollenbeck for the assistance with data analysis.

Conflict of interest

The authors have no conflicts of interest.

References

Allen, J.S., Damasio, H., Grabowski, T.J., 2002. Normal neuroanatomical variation in the human brain: an MRI-volumetric study. Am. J. Phys. Anthropol. 118, 341–358.

Allen, J.S., Bruss, J., Brown, C.K., Damasio, H., 2005. Normal neuroanatomical variation due to age: the major lobes and a parcellation of the temporal region. Neurobiol. Aging 26, 1245–1260 (discussion 1279–1282).

Andrews-Hanna, J.R., Snyder, A.Z., Vincent, J.L., Lustig, C., Head, D., Raichle, M.E., Buckner, R.L., 2007. Disruption of large-scale brain systems in advanced aging. Neuron 56, 924–935.

Arnold, S.E., Hyman, B.T., Flory, J., Damasio, A.R., Van Hoesen, G.W., 1991. The topographical and neuroanatomical distribution of neurofibrillary tangles and neuritic plaques in the cerebral cortex of patients with Alzheimer's disease. Cereb. Cortex 1, 103–116.

Arriagada, P.V., Marzloff, K., Hyman, B.T., 1992. Distribution of Alzheimer-type pathologic changes in nondemented elderly individuals matches the pattern in Alzheimer's disease. Neurology 42, 1681–1688.

Bakkour, A., Morris, J.C., Dickerson, B.C., 2009. The cortical signature of prodromal AD: regional thinning predicts mild AD dementia. Neurology 72, 1048–1055.

Becker, J.A., Hedden, T., Carmasin, J., Maye, J., Rentz, D.M., Putcha, D., Fischl, B., Greve, D.N., Marshall, G.A., Salloway, S., Marks, D., Buckner, R.L., Sperling, R.A., Johnson, K.A., 2011. Amyloid-beta associated cortical thinning in clinically normal elderly. Ann. Neurol. 69, 1032–1042.

Berg, L., McKeel Jr., D.W., Miller, J.P., Storandt, M., Rubin, E.H., Morris, J.C., Baty, J., Coats, M., Norton, J., Goate, A.M., Price, J.L., Gearing, M., Mirra, S.S., Saunders, A.M., 1998. Clinicopathologic studies in cognitively healthy aging and Alzheimer's disease: relation of histologic markers to dementia severity, age, sex, and apolipoprotein E genotype. Arch. Neurol. 55, 326–335.

Braak, H., Braak, E., 1991. Neuropathological stageing of Alzheimer-related changes. Acta Neuropathol. (Berl.) 82, 239–259.

Brickman, A.M., Habeck, C., Zarahn, E., Flynn, J., Stern, Y., 2007. Structural MRI covariance patterns associated with normal aging and neuropsychological functioning. Neurobiol. Aging 28, 284–295.

Brun, A., Gustafson, L., 1976. Distribution of cerebral degeneration in Alzheimer's disease. A clinico-pathological study. Arch. Psychiatr. Nervenkr. 223, 15–33.

Buckner, R.L., 2004. Memory and executive function in aging and AD: multiple factors that cause decline and reserve factors that compensate. Neuron 44, 195–208.

Buckner, R.L., Snyder, A.Z., Shannon, B.J., LaRossa, G., Sachs, R., Fotenos, A.F., Sheline, Y.I., Klunk, W.E., Mathis, C.A., Morris, J.C., Mintun, M.A., 2005. Molecular, structural, and functional characterization of Alzheimer's disease: evidence for a relationship between default activity, amyloid, and memory. J. Neurosci. 25, 7709–7717.

Chetelat, G., Landeau, B., Eustache, F., Mezenge, F., Viader, F., de la Sayette, V., Desgranges, B., Baron, J.C., 2005. Using voxel-based morphometry to map the structural changes associated with rapid conversion in MCI: a longitudinal MRI study. Neuroimage 27, 934–946.

Chetelat, G., Villemagne, V.L., Bourgeat, P., Pike, K.E., Jones, G., Ames, D., Ellis, K.A., Szoeke, C., Martins, R.N., O'Keefe, G.J., Salvado, O., Masters, C.L., Rowe, C.C., Australian Imaging B, Lifestyle Research G, 2010. Relationship between atrophy and beta-amyloid deposition in Alzheimer disease. Ann. Neurol. 67, 317–324.

Cohen, A.L., Fair, D.A., Dosenbach, N.U., Miezin, F.M., Dierker, D., Van Essen, D.C., Schlaggar, B.L., Petersen, S.E., 2008. Defining functional areas in individual human brains using resting functional connectivity MRI. Neuroimage 41, 45–57.

Corbetta, M., Shulman, G.L., 2002. Control of goal-directed and stimulus-driven attention in the brain. Nat. Rev. Neurosci. 3, 201–215.

Craig, A.D., 2002. How do you feel? Interoception: the sense of the physiological condition of the body. Nat. Rev. Neurosci. 3, 655–666.

Dale, A.M., Fischl, B., Sereno, M.I., 1999. Cortical surface-based analysis. I. Segmentation and surface reconstruction. Neuroimage 9, 179–194.

Dickerson, B.C., Feczko, E., Augustinack, J.C., Pacheco, J., Morris, J.C., Fischl, B., Buckner, R.L., 2009a. Differential effects of aging and Alzheimer's disease on medial temporal lobe cortical thickness and surface area. Neurobiol. Aging 30, 432–440.

Dickerson, B.C., Bakkour, A., Salat, D.H., Feczko, E., Pacheco, J., Greve, D.N., Grodstein, F., Wright, C.I., Blacker, D., Rosas, H.D., Sperling, R.A., Atri, A., Growdon, J.H., Hyman, B.T., Morris, J.C., Fischl, B., Buckner, R.L., 2009b. The cortical signature of Alzheimer's disease: regionally specific cortical thinning relates to symptom severity in very mild to mild AD dementia and is detectable in asymptomatic amyloid-positive individuals. Cereb. Cortex 19, 497–510.

Dickerson, B.C., Stoub, T., Shah, R.C., Sperling, R.A., Killiany, R.J., Albert, M.S., Hyman, B.T., Blacker, D., deToledo-Morrell, L., 2011. Alzheimer-signature MRI biomarker predicts AD dementia in cognitively normal adults. Neurology 76, 1395–1402.

Dickerson, B.C., Wolk, D.A., On behalf of the Alzheimer's Disease Neuroimaging I, 2012. MRI cortical thickness biomarker predicts AD-like CSF and cognitive decline in normal adults. Neurology 78, 84–90.

Driscoll, I., Davatzikos, C., An, Y., Wu, X., Shen, D., Kraut, M., Resnick, S.M., 2009. Longitudinal pattern of regional brain volume change differentiates normal aging from MCI. Neurology 72, 1906–1913.

Fagan, A.M., Mintun, M.A., Mach, R.H., Lee, S.Y., Dence, C.S., Shah, A.R., LaRossa, G.N., Spinner, M.L., Klunk, W.E., Mathis, C.A., DeKosky, S.T., Morris, J.C., Holtzman, D.M., 2006. Inverse relation between in vivo amyloid imaging load and cerebrospinal fluid Abeta42 in humans. Ann. Neurol. 59, 512–519.

Fischl, B., Dale, A.M., 2000. Measuring the thickness of the human cerebral cortex from magnetic resonance images. Proc. Natl. Acad. Sci. U. S. A. 97, 11050–11055.

Fischl, B., Sereno, M.I., Dale, A.M., 1999. Cortical surface-based analysis. II: inflation, flattening, and a surface-based coordinate system. Neuroimage 9, 195–207.

Fischl, B., Liu, A., Dale, A.M., 2001. Automated manifold surgery: constructing geometrically accurate and topologically correct models of the human cerebral cortex. IEEE Trans. Med. Imaging 20, 70–80.

Fischl, B., Salat, D.H., Busa, E., Albert, M., Dieterich, M., Haselgrove, C., van der Kouwe, A., Killiany, R., Kennedy, D., Klaveness, S., Montillo, A., Makris, N., Rosen, B., Dale, A.M., 2002. Whole brain segmentation: automated labeling of neuroanatomical structures in the human brain. Neuron 33, 341–355.

Fjell, A.M., Walhovd, K.B., Fennema-Notestine, C., McEvoy, L.K., Hagler, D.J., Holland, D., Brewer, J.B., Dale, A.M., 2009a. One-year brain atrophy evident in healthy aging. J. Neurosci. 29, 15223–15231.

Fjell, A.M., Westlye, L.T., Amlien, I., Espeseth, T., Reinvang, I., Raz, N., Agartz, I., Salat, D.H., Greve, D.N., Fischl, B., Dale, A.M., Walhovd, K.B., 2009b. High consistency of regional cortical thinning in aging across multiple samples. Cereb. Cortex 19, 2001–2012.

Fjell, A.M., Amlien, I.K., Westlye, L.T., Stenset, V., Fladby, T., Skinningsrud, A., Eilsertsen, D.E., Bjornerud, A., Walhovd, K.B., 2010a. CSF biomarker pathology correlates with a medial temporo-parietal network affected by very mild to moderate Alzheimer's disease but not a fronto-striatal network affected by healthy aging. Neuroimage 49, 1820–1830.

Fjell, A.M., Walhovd, K.B., Fennema-Notestine, C., McEvoy, L.K., Hagler, D.J., Holland, D., Blennow, K., Brewer, J.B., Dale, A.M., Alzheimer's Disease Neuroimaging I, 2010b. Brain atrophy in healthy aging is related to CSF levels of Abeta1–42. Cereb. Cortex 20, 2069–2079.

Fotenos, A.F., Mintun, M.A., Snyder, A.Z., Morris, J.C., Buckner, R.L., 2008. Brain volume decline in aging: evidence for a relation between socioeconomic status, preclinical Alzheimer disease, and reserve. Arch. Neurol. 65, 113–120.

Freeman, S.H., Kandel, R., Cruz, L., Rozkalne, A., Newell, K., Frosch, M.P., Hedley-Whyte, E.T., Locascio, J.J., Lipsitz, L.A., Hyman, B.T., 2008. Preservation of neuronal number despite age-related cortical brain atrophy in elderly subjects without Alzheimer disease. J. Neuropathol. Exp. Neurol. 67, 1205–1212.

Gabrieli, J.D., Poldrack, R.A., Desmond, J.E., 1998. The role of left prefrontal cortex in language and memory. Proc. Natl. Acad. Sci. U. S. A. 95, 906–913.

Good, C.D., Johnsrude, I.S., Ashburner, J., Henson, R.N., Friston, K.J., Frackowiak, R.S., 2001. A voxel-based morphometric study of ageing in 465 normal adult human brains. Neuroimage 14, 21–36.

Han, X., Jovicich, J., Salat, D., van der Kouwe, A., Quinn, B., Czanner, S., Busa, E., Pacheco, J., Albert, M., Killiany, R., Maguire, P., Rosas, D., Makris, N., Dale, A., Dickerson, B., Fischl, B., 2006. Reliability of MRI-derived measurements of human cerebral cortical thickness: the effects of field strength, scanner upgrade and manufacturer. Neuroimage 32, 180–194.

Head, D., Snyder, A.Z., Girton, L.E., Morris, J.C., Buckner, R.L., 2005. Frontal-hippocampal double dissociation between normal aging and Alzheimer's disease. Cereb. Cortex 15, 732–739.

Hedden, T., Gabrieli, J.D., 2004. Insights into the ageing mind: a view from cognitive neuroscience. Nat. Rev. Neurosci. 5, 87–96.

Hulette, C.M., Welsh-Bohmer, K.A., Murray, M.G., Saunders, A.M., Mash, D.C., McIntyre, L.M., 1998. Neuropathological and neuropsychological changes in "normal" aging: evidence for preclinical Alzheimer disease in cognitively normal individuals. J. Neuropathol. Exp. Neurol. 57, 1168–1174.

Jack Jr., C.R., Knopman, D.S., Weigand, S.D., Wiste, H.J., Vemuri, P., Lowe, V., Kantarci, K., Gunter, J.L., Senjem, M.L., Ivnik, R.J., Roberts, R.O., Rocca, W.A., Boeve, B.F., Petersen, R.C., 2012. An operational approach to National Institute on Aging–Alzheimer's Association criteria for preclinical Alzheimer disease. Ann. Neurol. 71, 765–775.

Jacobs, B., Driscoll, L., Schall, M., 1997. Life-span dendritic and spine changes in areas 10 and 18 of human cortex: a quantitative Golgi study. J. Comp. Neurol. 386, 661–680.

Jernigan, T.L., Salmon, D.P., Butters, N., Hesselink, J.R., 1991a. Cerebral structure on MRI, part II: specific changes in Alzheimer's and Huntington's diseases. Biol. Psychiatry 29, 68–81.

Jernigan, T.L., Archibald, S.L., Berhow, M.T., Sowell, E.R., Foster, D.S., Hesselink, J.R., 1991b. Cerebral structure on MRI, part I: localization of age-related changes. Biol. Psychiatry 29, 55–67.

Jernigan, T.L., Archibald, S.L., Fennema-Notestine, C., Gamst, A.C., Stout, J.C., Bonner, J., Hesselink, J.R., 2001. Effects of age on tissues and regions of the cerebrum and cerebellum. Neurobiol. Aging 22, 581–594.

Johnson, D.K., Storandt, M., Morris, J.C., Langford, Z.D., Galvin, J.E., 2008. Cognitive profiles in dementia: Alzheimer disease vs healthy brain aging. Neurology 71, 1783–1789.

Kalpouzos, G., Chetelat, G., Baron, J.C., Landeau, B., Mevel, K., Godeau, C., Barre, L., Constans, J.M., Viader, F., Eustache, F., Desgranges, B., 2009. Voxel-based mapping of brain gray matter volume and glucose metabolism profiles in normal aging. Neurobiol. Aging 30, 112–124.

Kanne, S.M., Balota, D.A., Storandt, M., McKeel Jr., D.W., Morris, J.C., 1998. Relating anatomy to function in Alzheimer's disease: neuropsychological profiles predict regional neuropathology 5 years later. Neurology 50, 979–985.

Kennedy, K.M., Erickson, K.I., Rodrigue, K.M., Voss, M.W., Colcombe, S.J., Kramer, A.F., Acker, J.D., Raz, N., 2009. Age-related differences in regional brain volumes: a comparison of optimized voxel-based morphometry to manual volumetry. Neurobiol. Aging 30, 1657–1676.

Klunk, W.E., et al., 2004. Imaging brain amyloid in Alzheimer's disease with Pittsburgh Compound-B. Ann. Neurol. 55, 306–319.

Kuperberg, G.R., Broome, M.R., McGuire, P.K., David, A.S., Eddy, M., Ozawa, F., Goff, D., West, W.C., Williams, S.C., van der Kouwe, A.J., Salat, D.H., Dale, A.M., Fischl, B., 2003. Regionally localized thinning of the cerebral cortex in schizophrenia. Arch. Gen. Psychiatry 60, 878–888.

Lemaitre, H., Crivello, F., Grassiot, B., Alperovitch, A., Tzourio, C., Mazoyer, B., 2005. Age- and sex-related effects on the neuroanatomy of healthy elderly. Neuroimage 26, 900–911.

Lerch, J.P., Pruessner, J.C., Zijdenbos, A., Hampel, H., Teipel, S.J., Evans, A.C., 2005. Focal decline of cortical thickness in Alzheimer's disease identified by computational neuroanatomy. Cereb. Cortex 15, 995–1001.

Lindenberger, U., Baltes, P.B., 1994. Sensory functioning and intelligence in old age: a strong connection. Psychol. Aging 9, 339–355.

Marcus, D.S., Wang, T.H., Parker, J., Csernansky, J.G., Morris, J.C., Buckner, R.L., 2007. Open Access Series of Imaging Studies (OASIS): cross-sectional MRI data in young, middle aged, nondemented, and demented older adults. J. Cogn. Neurosci. 19, 1498–1507.

McDonald, C.R., McEvoy, L.K., Gharapetian, L., Fennema-Notestine, C., Hagler Jr., D.J., Holland, D., Koyama, A., Brewer, J.B., Dale, A.M., Alzheimer's Disease Neuroimaging I, 2009. Regional rates of neocortical atrophy from normal aging to early Alzheimer disease. Neurology 73, 457–465.

McKhann, G., Drachman, D., Folstein, M., Katzman, R., Price, D., Stadlan, E.M., 1984. Clinical diagnosis of Alzheimer's disease: report of the NINCDS-ADRDA Work Group under the auspices of Department of Health and Human Services Task Force on Alzheimer's Disease. Neurology 34, 939–944.

Mintun, M.A., Larossa, G.N., Sheline, Y.I., Dence, C.S., Lee, S.Y., Mach, R.H., Klunk, W.E., Mathis, C.A., DeKosky, S.T., Morris, J.C., 2006. [11C]PIB in a nondemented population: potential antecedent marker of Alzheimer disease. Neurology 67, 446–452.

Mormino, E.C., Kluth, J.T., Madison, C.M., Rabinovici, G.D., Baker, S.L., Miller, B.L., Koeppe, R.A., Mathis, C.A., Weiner, M.W., Jagust, W.J., Alzheimer's Disease Neuroimaging I, 2009. Episodic memory loss is related to hippocampal-mediated beta-amyloid deposition in elderly subjects. Brain 132, 1310–1323.

Morris, J.C., 1993. The Clinical Dementia Rating (CDR): current version and scoring rules. Neurology 43, 2412–2414.

Morris, J.C., Ernesto, C., Schafer, K., Coats, M., Leon, S., Sano, M., Thal, L.J., Woodbury, P., 1997. Clinical dementia rating training and reliability in multicenter studies: the Alzheimer's Disease Cooperative Study experience. Neurology 48, 1508–1510.

Morris, J.C., Roe, C.M., Grant, E.A., Head, D., Storandt, M., Goate, A.M., Fagan, A.M., Holtzman, D.M., Mintun, M.A., 2009. Pittsburgh compound B imaging and prediction of progression from cognitive normality to symptomatic Alzheimer disease. Arch. Neurol. 66, 1469–1475.

Ohnishi, T., Matsuda, H., Tabira, T., Asada, T., Uno, M., 2001. Changes in brain morphology in Alzheimer disease and normal aging: is Alzheimer disease an exaggerated aging process? AJNR Am. J. Neuroradiol. 22, 1680–1685.

Pakkenberg, B., Gundersen, H.J., 1997. Neocortical neuron number in humans: effect of sex and age. J. Comp. Neurol. 384, 312–320.

Price, J.L., Morris, J.C., 1999. Tangles and plaques in nondemented aging and "preclinical" Alzheimer's disease. Ann. Neurol. 45, 358–368.

Price, J.L., Davis, P.B., Morris, J.C., White, D.L., 1991. The distribution of tangles, plaques and related immunohistochemical markers in healthy aging and Alzheimer's disease. Neurobiol. Aging 12, 295–312.

Price, J.L., et al., 2009. Neuropathology of nondemented aging: presumptive evidence for preclinical Alzheimer disease. Neurobiol. Aging 30, 1026–1036.

Raji, C.A., Lopez, O.L., Kuller, L.H., Carmichael, O.T., Becker, J.T., 2009. Age, Alzheimer disease, and brain structure. Neurology 73, 1899–1905.

Raz, N., Rodrigue, K.M., 2006. Differential aging of the brain: patterns, cognitive correlates and modifiers. Neurosci. Biobehav. Rev. 30, 730–748.

Raz, N., Gunning, F.M., Head, D., Dupuis, J.H., McQuain, J., Briggs, S.D., Loken, W.J., Thornton, A.E., Acker, J.D., 1997. Selective aging of the human cerebral cortex observed in vivo: differential vulnerability of the prefrontal gray matter. Cereb. Cortex 7, 268–282.

Raz, N., Gunning-Dixon, F.M., Head, D., Dupuis, J.H., Acker, J.D., 1998. Neuroanatomical correlates of cognitive aging: evidence from structural magnetic resonance imaging. Neuropsychology 12, 95–114.

Raz, N., Rodrigue, K.M., Head, D., Kennedy, K.M., Acker, J.D., 2004. Differential aging of the medial temporal lobe: a study of a five-year change. Neurology 62, 433–438.

Raz, N., Lindenberger, U., Rodrigue, K.M., Kennedy, K.M., Head, D., Williamson, A., Dahle, C., Gerstorf, D., Acker, J.D., 2005. Regional brain changes in aging healthy adults: general trends, individual differences and modifiers. Cereb. Cortex 15, 1676–1689.

Resnick, S.M., Pham, D.L., Kraut, M.A., Zonderman, A.B., Davatzikos, C., 2003. Longitudinal magnetic resonance imaging studies of older adults: a shrinking brain. J. Neurosci. 23, 3295–3301.

Rodrigue, K.M., Raz, N., 2004. Shrinkage of the entorhinal cortex over five years predicts memory performance in healthy adults. J. Neurosci. 24, 956–963.

Rodrigue, K.M., Kennedy, K.M., Devous Sr., M.D., Rieck, J.R., Hebrank, A.C., Diaz-Arrastia, R., Mathews, D., Park, D.C., 2012. Beta-amyloid burden in healthy aging: regional distribution and cognitive consequences. Neurology 78, 387–395.

Rosas, H.D., Liu, A.K., Hersch, S., Glessner, M., Ferrante, R.J., Salat, D.H., van der Kouwe, A., Jenkins, B.G., Dale, A.M., Fischl, B., 2002. Regional and progressive thinning of the cortical ribbon in Huntington's disease. Neurology 58, 695–701.

Salat, D.H., Buckner, R.L., Snyder, A.Z., Greve, D.N., Desikan, R.S., Busa, E., Morris, J.C., Dale, A.M., Fischl, B., 2004. Thinning of the cerebral cortex in aging. Cereb. Cortex 14, 721–730.

Sato, K., Taki, Y., Fukuda, H., Kawashima, R., 2003. Neuroanatomical database of normal Japanese brains. Neural Netw. 16, 1301–1310.

Scahill, R.I., Schott, J.M., Stevens, J.M., Rossor, M.N., Fox, N.C., 2002. Mapping the evolution of regional atrophy in Alzheimer's disease: unbiased analysis of fluid-registered serial MRI. Proc. Natl. Acad. Sci. U. S. A. 99, 4703–4707.

Smith, C.D., Chebrolu, H., Wekstein, D.R., Schmitt, F.A., Markesbery, W.R., 2007. Age and gender effects on human brain anatomy: a voxel-based morphometric study in healthy elderly. Neurobiol. Aging 28, 1075–1087.

Sperling, R.A., et al., 2011. Toward defining the preclinical stages of Alzheimer's disease: recommendations from the National Institute on Aging and the Alzheimer's Association workgroup. Alzheimers Dement. 7, 280–292.

Stuss, D.T., Alexander, M.P., 2007. Is there a dysexecutive syndrome? Philos. Trans. R. Soc. Lond. B Biol. Sci. 362, 901–915.

Taki, Y., Goto, R., Evans, A., Zijdenbos, A., Neelin, P., Lerch, J., Sato, K., Ono, S., Kinomura, S., Nakagawa, M., Sugiura, M., Watanabe, J., Kawashima, R., Fukuda, H., 2004. Voxel-based morphometry of human brain with age and cerebrovascular risk factors. Neurobiol. Aging 25, 455–463.

Thompson, P.M., Mega, M.S., Woods, R.P., Zoumalan, C.I., Lindshield, C.J., Blanton, R.E., Moussai, J., Holmes, C.J., Cummings, J.L., Toga, A.W., 2001. Cortical change in Alzheimer's disease detected with a disease-specific population-based brain atlas. Cereb. Cortex 11, 1–16.

Tisserand, D.J., Pruessner, J.C., Sanz Arigita, E.J., van Boxtel, M.P., Evans, A.C., Jolles, J., Uylings, H.B., 2002. Regional frontal cortical volumes decrease differentially in aging: an MRI study to compare volumetric approaches and voxel-based morphometry. Neuroimage 17, 657–669.

Troncoso, J.C., Martin, L.J., Dal Forno, G., Kawas, C.H., 1996. Neuropathology in controls and demented subjects from the Baltimore Longitudinal Study of Aging. Neurobiol. Aging 17, 365–371.

Vincent, J.L., Kahn, I., Snyder, A.Z., Raichle, M.E., Buckner, R.L., 2008. Evidence for a frontoparietal control system revealed by intrinsic functional connectivity. J. Neurophysiol. 100, 3328–3342.

von Economo, C., 2009. Cellular Structure of the Human Cerebral Cortex. Karger AG, Basel.

Walhovd, K.B., Fjell, A.M., Reinvang, I., Lundervold, A., Dale, A.M., Eilertsen, D.E., Quinn, B.T., Salat, D., Makris, N., Fischl, B., 2005. Effects of age on volumes of cortex, white matter and subcortical structures. Neurobiol. Aging 26, 1261–1270 (discussion 1275–1268).

Walhovd, K.B., Westlye, L.T., Amlien, I., Espeseth, T., Reinvang, I., Raz, N., Agartz, I., Salat, D.H., Greve, D.N., Fischl, B., Dale, A.M., Fjell, A.M., 2009. Consistent neuroanatomical age-related volume differences across multiple samples. Neurobiol. Aging 32, 916–932.

Whitwell, J.L., Shiung, M.M., Przybelski, S.A., Weigand, S.D., Knopman, D.S., Boeve, B.F., Petersen, R.C., Jack Jr., C.R., 2008. MRI patterns of atrophy associated with progression to AD in amnestic mild cognitive impairment. Neurology 70, 512–520.

Wonderlick, J.S., Ziegler, D.A., Hosseini-Varnamkhasti, P., Locascio, J.J., Bakkour, A., van der Kouwe, A., Triantafyllou, C., Corkin, S., Dickerson, B.C., 2009. Reliability of MRI-derived cortical and subcortical morphometric measures: effects of pulse sequence, voxel geometry, and parallel imaging. Neuroimage 44, 1324–1333.